Journal of Pharmacology and Toxicology

ISSN 1816-496X

Academic Journals Inc.

www.academicjournals.com

Journal of Pharmacology and Toxicology 1 (5): 447-455, 2006
ISSN 1816-496X

Molecular Modelling Analysis of the Metabolism of Isoniazid

Fazlul Huq
School of Biomedical Sciences, Faculty of Health Sciences,
The University of Sydney, Australia

Abstract: Isoniazid is the cornerstone of therapy against tuberculosis which is a global health problem of increasing dimension. Isoniazid is metabolized in the liver by acetylation and hydroxylation. Molecular modelling analyses based on molecular mechanics, semi-empirical (PM3) and DFT (at B3LYP/6-31G* level) calculations show that isoniazid and its metabolites differ to some extent in their solvation energy, surface charge distribution, dipole moment, thermodynamic stability and kinetic lability. The metabolites hydrazine and acetylhydrazine are believed to be responsible for isoniazid induced liver toxicity. However, the results of molecular modelling analyses show that both the metabolites are kinetically inert. It is possible that these are spontaneously converted to more reactive metabolites pyruvate hydrazone and 1,4,5,6-tetrahydro-6-oxo-3-pyridazine carboxylic acid. The charged nature of the surface of isoniazid and its metabolites indicates that the compounds may interact with biomolecules electrically. It also explains why the molecules are soluble in water.

Key words: Isoniazid, tuberculosis, acetylation, molecular modelling

Introduction

Tuberculosis (TB) caused by *Mycobacterium tuberculosis* is a global health problem of increasing dimension. It is also a marker of social inequity and serious impediment to economic development (WHO Report, 2002). In 1990, 8 million new cases were reported with 95% of them being in developing countries where co-infection with HIV is common (Kochi, 1991). Although effective chemotherapy has been used to treat TB for over fifty years, projections based on recent research indicate that TB will remain as one of the world's top ten causes of adult mortality in the year 2020 (Dye *et al*., 1999, Arnadottir, 2001).

Isoniazid (INH) is the cornerstone of most therapeutic regimens used for the treatment of TB and the only drug for prophylaxis against early infection (Smith and Reynard, 1992). INH is bactericidal against growing organisms and bacteriostatic against dominant strains. It can penetrate human cell membranes and is active against intracellular organisms. INH is readily absorbed following oral administration.

Adverse effects of INH include nausea, vomiting, diarrhoea, fever and maculopapular rash. Neurotoxicity can also be seen with INH. It can cause vitamin B_6 deficiency by forming hydrazones that inhibit its conversion to pyridoxal phosphate or inactivate it (Smith and Reynard, 1992). Because vitamin B_6 is a cofactor for the production of neurotransmitters, neuropathy results. Clinical manifestations include paresthesias and peripheral neuropathy and may also extend to sensory or motor dysfunction. INH also produces hepatocellular dysfunction in approximately 15% of recipients (Smith and Reynard, 1992). INH is contraindicated in patients who develop severe hypersensitivity reactions, including drug-induced hepatitis. It is also contraindicated for patients with previous INH-induced hepatitic injury.

INH is metabolized in the liver by acetylation and hydroxylation. The rate of acetylation is bimodal in the population. Genetically polymorphic enzyme arylamine *N*-acetyltransferase type 2 (NAT2), a hepatitic phase II drug-metabolizing enzyme, is involved in acetylation. Individuals can be classified as rapid acetylators or slow acetylators depending on their INH *N*-acetylation capacity (Evans *et al*., 1960). Approximately half the population in the USA is estimated to acetylate INH rapidly. Certain other populations have widely different rates (Eskimos 95%, Egyptians 17% rapid acetylators). The large majority of metabolites of INH are excreted in the urine. A small fraction of unchanged drug is also cleared by the kidney. Current literature indicates not only INH concentrations but also efficacy and toxicity due to INH are linked to the activity of NAT2 enzyme. It is also well established that slow acetylators are more likely to develop polyneuropathy during INH therapy if no vitamin B_6 is administered (Kinzig-Schippers *et al*., 2005). Slow acetylators are at a greater risk to develop hepatotoxicity than rapid acetylators (Clark, 1985; Eichelbaum *et al*., 1992). The association between NAT2 genotypes and severe liver injury has been found in Japanese TB patients treated with standard dose of INH plus ifamin (Kinzig-Schippers *et al*., 2005).

N-acetylation of INH produces *N*-acetylisoniazid (NAINH). Two other metabolites of INH are hydrazine (HD) and acteylhydrazine (AcHD). AcHD is actually the major metabolite of INH. HD and AcHD can be metabolized to produce diacetylhdrazone (DAHD) (Huq, 2006a). HD can also produce nitrogen, pyruvate hydrazone (PH) and 1,4,5,6-tetrahydro-6-oxo-3-pyridazine carboxylic acid (THOPC). Recent studies indicate that INH-induced liver toxicity is caused by AcHD (Richards *et al*., 2004). Figure 1 gives the metabolic pathway for INH.

In this study, molecular modelling analyses have been carried out using the programs HyperChem 7.0 (HyperChem, 2002) and Spartan '02 (Spartan, 2002) to investigate the relative stability of INH and its metabolites with the aim of providing a better understanding on the toxicity due to INH and its metabolites. The work was carried out in the School of Biomedical Sciences, The University of Sydney during December 2005 to April 2006.

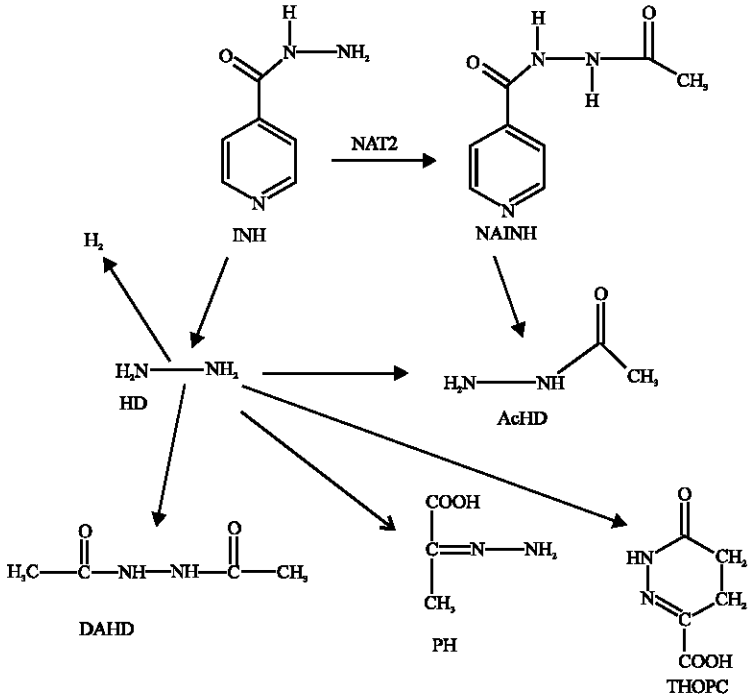

Fig. 1: Proposed metabolic pathways for INH and its metabolites (Kinzig-Schippers *et al*., 2005)

Computational Methods

The geometries of INH and its metabolites NAINH, AcHD, HD, DAHD, PH and THOPC have been optimised based on molecular mechanics, semi-empirical and DFT calculations, using the molecular modelling programs HyperChem 7.0 and Spartan '02. Molecular mechanics calculations were carried out using MMFF force field. Semi-empirical calculations were carried out using the routine PM3. DFT calculations were carried using the program Spartan '02 at B3LYP/6-31G* level. In optimization calculations, a RMS gradient of 0.001 was set as the terminating condition.

For the optimised structures, single point calculations were carried to give heat of formation, enthalpy, entropy, free energy, dipole moment, solvation energy, surface area, volume, energies for HOMO and LUMO. The order of calculations: molecular mechanics followed by semi-empirical followed by DFT minimized the chances of the structures being trapped in local minima rather reaching global minima. To further check whether the global minimum was reached, some calculations were carried out with improvable structures. It was found that when the stated order was followed, structures corresponding to global minimum or close to that were reached in most cases. Although RMS gradient of 0.001 may not be sufficiently small for vibrational analysis, it is believed to be sufficiently low for calculations associated with electronic energy levels.

Results and Discussion

Table 1 gives the total energy, heat of formation as per PM3 calculation, enthalpy, entropy, free energy, dipole moment, energies of HOMO and LUMO as per both PM3 and DFT calculations for INH and its metabolites NAINH, AcHD, HD, DAHD, PH and THOPC. Figure 2-8 give the regions of negative electrostatic potential (greyish-white envelopes) in (a), HOMOs (where red indicates HOMOs with high electron density) in (b), LUMOs in © and surface charges (where red indicates negative, blue indicates positive and green indicates neutral) in (d) as applied to the optimised structures of INH and its metabolites NAINH, AcHD, HD, DAHD, PH and THOPC, respectively, as per DFT calculations.

The molecules are found to differ in the calculated values of total energy, heat of formation, solvation energy, surface area, volume and dipole moment. After HD, INH has the second highest positive heat of formation (much greater than that of NAINH) and second largest total energy from PM3 calculations. Since the entropy of NAINH is greater than that of INH (114.32 cal mol^{-1} K^{-1} for the former and 92.46 cal mol^{-1} K^{-1} for the latter from DFT calculations), it is likely that Gibb's free energy change (ΔG) defined by the equation: $\Delta G = \Delta H - T\Delta S$ for the reaction: INH _→ NAINH would be negative and if this is so the conversion of INH to NAINH would occur spontaneously. That the highest heat of formation is found for HD (even though it has a smaller molecular size) may also mean that it would be most unstable thermodynamically. However, the large LUMO-HOMO energy difference (7.54 eV from DFT calculations) makes the molecule kinetically inert. More about LUMO-HOMO energy difference will be considered later. The large positive heat of formation of HD also means that it would spontaneously change to more labile metabolites PH and THOPC both of which have large negative heats of formation.

The calculated solvation energies of INH, NAINH, AcHD, HD, DAHD, PH and THOPC from PM3 calculations in kcal mol^{-1} are respectively -10.61, -13.92, -7.92, -9.02, -12.41, -7.98 and -12.99, respectively and their dipole moments from DFT calculations are 1.87, 3.44, 3.60, 0, 5.52, 0.74 and 2.04, respectively. The values show that the compounds would differ only to a limited extent in their solubility in water. Although HD has a zero dipole moment, negative solvation energy value of -9.02 kcal mol^{-1} indicates that the compound would be quite soluble in water. The results point to the complexity of the process of solution in water where hydrogen bonding, solvent-induced ionization and resonance stabilization are often found to occur (Huq, 2006).

Table 1: Calculated thermodynamic and other parameters of INH and its metabolites

Molecule	Calculation type	Total energy (kcal mol^{-1}/ atomic unit*)	Heat of formation (kcal mol^{-1})	Enthalpy (kcal mol^{-1} K^{-1})	Entropy (cal mol^{-1} K^{-1})	Solvation energy (kcal mol^{-1} K^{-1})	Free energy (kcal mol^{-1})
INH	PM3	9.12	19.72	87.40	94.54	-10.61	59.22
	DFT	-472.32		89.36	92.46	-10.00	61.80
NAINH	PM3	-37.44	-23.51	112.29	111.81	-13.92	78.96
	DFT	-624.96		114.81	114.32	-12.77	80.72
AcHD	PM3	-29.07	-21.15	66.71	75.01	-7.92	44.35
	DFT	-264.54		61.21	76.79	-8.02	38.32
HD	PM3	16.75	20.65	35.33	55.61	-9.02	18.75
	DFT	-111.86		35.62	57.89	-5.47	18.36
DAHD	PM3	-72.23	-59.82	85.13	91.23	-12.41	57.93
	DFT	-417.21		86.88	95.06	-10.56	58.53
PH	PM3	-72.23	-59.82	75.75	76.20	-7.98	53.03
	DFT	-377.87		68.28	82.79	-7.59	43.59
THOPC	PM3	-109.51	-96.53	79.49	94.13	-12.99	51.43
	DFT	-529.33		80.51	91.45	-11.19	53.25

Molecule	Calculation type	Dipole moment (debye)	Surface area (Å^2)	Volume (Å^3)	HOMO (eV)	LUMO (eV)	LUMO-HOMO (eV)
INH	PM3	1.32	162.97	136.87	-10.09	-0.62	9.47
	DFT	1.87	160.24	136.01	-7.13	-1.64	5.49
NAINH	PM3	2.46	209.22	179.05	-10.08	-0.63	9.45
	DFT	3.44	206.50	177.56	-7.08	-1.58	5.50
AcHD	PM3	3.19	102.89	76.72	-9.43	0.72	10.15
	DFT	3.60	104.54	76.87	-6.61	0.77	7.38
HD	PM3	0.00	58.44	34.96	-9.02	2.76	10.06
	DFT	0.00	59.49	35.63	-5.47	2.07	7.54
DAHD	PM3	4.98	145.04	118.22	-10.09	0.14	10.23
	DFT	5.52	148.99	118.22	-6.84	0.21	7.05
PH	PM3	0.37	126.33	97.36	-10.09	0.14	10.23
	DFT	0.74	122.68	96.25	-6.19	-1.20	4.99
THOPC	PM3	2.98	150.78	126.09	-10.17	-0.95	9.22
	DFT	2.04	148.67	125.32	-7.34	-2.16	5.18

* in atomic units from DFT calculations

The LUMO-HOMO energy differences for INH and its metabolites (obtained from DFT calculations) range from 4.99 to 7.38 eV, indicating that the compounds would vary significantly in their kinetic lability. PH (a direct metabolite of HD and indirectly a metabolite of INH) has the smallest LUMO-HOMO energy difference (4.99 eV) indicating that it would be most labile whereas (as noted earlier) HD has the largest LUMO-HOMO energy difference (7.54 eV) indicating that it would be least labile kinetically.

Since kinetic factor rather than t he thermodynamic ones is considered to be the key determinant of toxicity of xenbiotics and their metabolites (as biochemical reactions may be coupled such that the overall free energy for the process is negative so that the overall process would be spontaneous), it is possible that PH and THOPC may be more toxic. It was noted earlier that liver toxicity due to INH is associated with AcHD. However, AcHD is expected to be kinetically inert as it has a large LUMO-HOMO energy difference. Thus, the toxicity due to AcHD cannot be explained from kinetic consideration. It is however possible that the likely toxic metabolites PH and THOPC may be produced spontaneously from both HD and AcHD. It should also be noted that other factors such as molecular size, shape, nature of molecular surface (in terms of variable as polarity and hydrophobicity) and electrostatic potential may be playing key roles in determining toxicity.

In the case of INH, the electrostatic potential is found to be more negative around the carbonyl oxygen atom, nitrogen atom of the pyridine ring and the primary amino nitrogen atom of the hydrazine side chain, indicating that the positions may be subject to electrophilic attack; in the case of NAINH

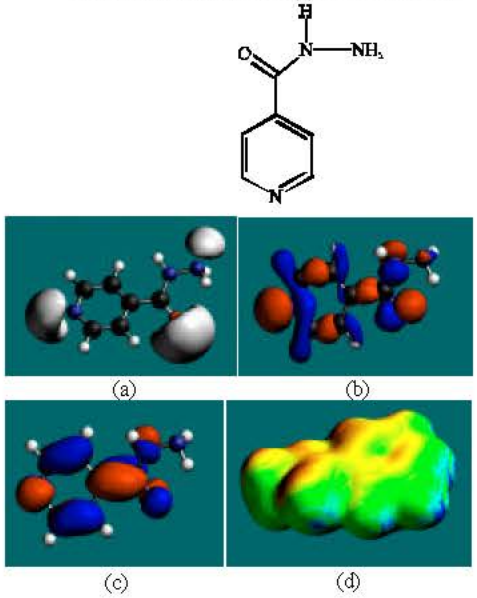

Fig. 2: Structure of INH giving the electrostatic potential in (a), HOMOs in (b), LUMOs in (c) and surface electric charges (where red indicates negative, blue indicates positive and green indicates neutral) in (d)

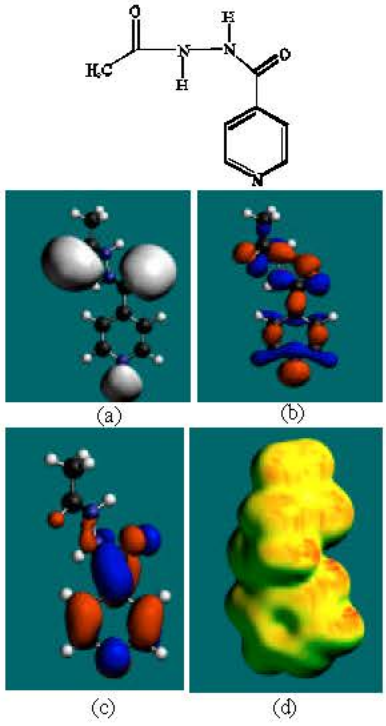

Fig. 3: Structure of NAINH giving the electrostatic potential in (a), HOMOs in (b), LUMOs in (c) and surface electric charges (where red indicates negative, blue indicates positive and green indicates neutral) in (d)

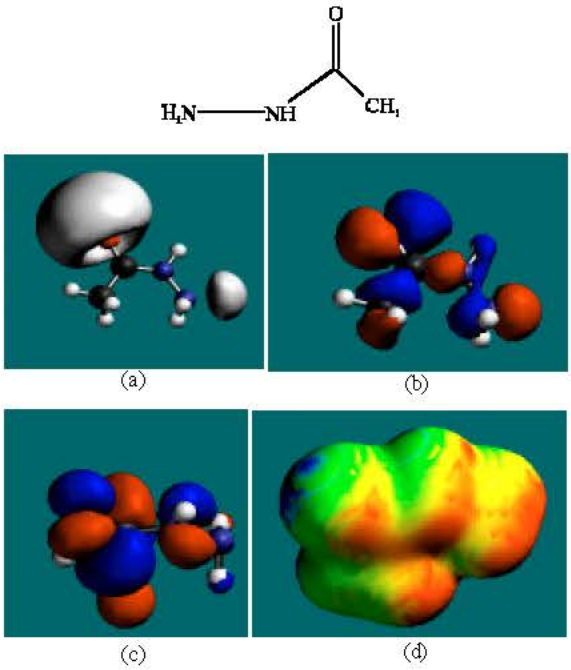

Fig. 4: Structure of AcHD giving the electrostatic potential in (a), HOMOs in (b), LUMOs in (c) and surface electric charges (where red indicates negative, blue indicates positive and green indicates neutral) in (d)

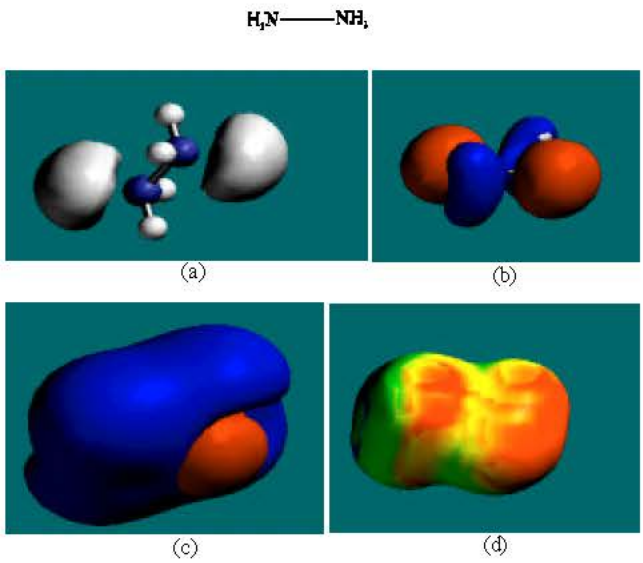

Fig. 5: Structure of HD giving the electrostatic potential in (a), HOMOs in (b), LUMOs in (c) and surface electric charges (where red indicates negative, blue indicates positive and green indicates neutral) in (d)

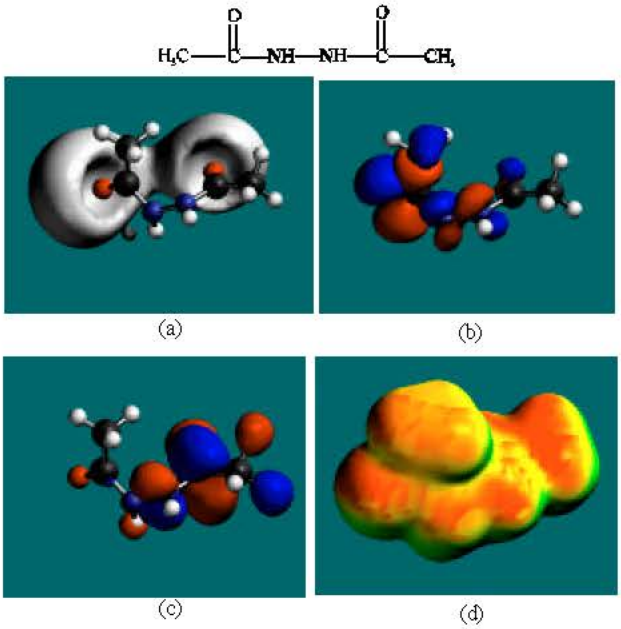

Fig. 6: Structure of DAHD giving the electrostatic potential in (a), HOMOs in (b), LUMOs in (c) and surface electric charges (where red indicates negative, blue indicates positive and green indicates neutral) in (d)

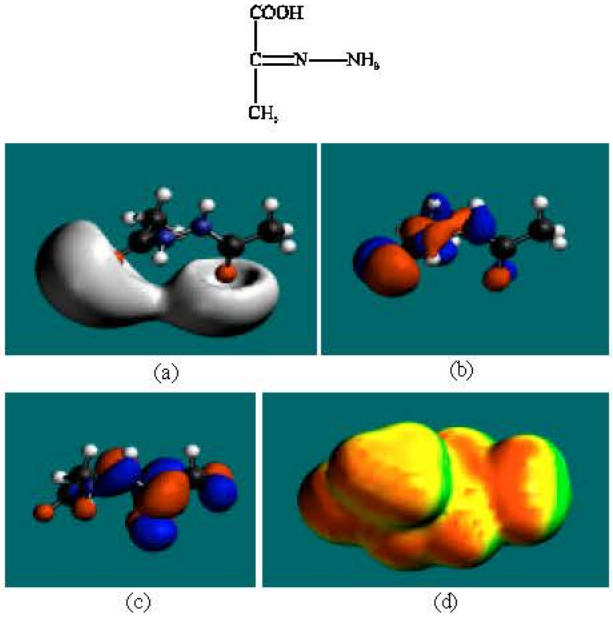

Fig. 7: Structure of PH giving the electrostatic potential in (a), HOMOs in (b), LUMOs in (c) and surface electric charges (where red indicates negative, blue indicates positive and green indicates neutral) in (d)

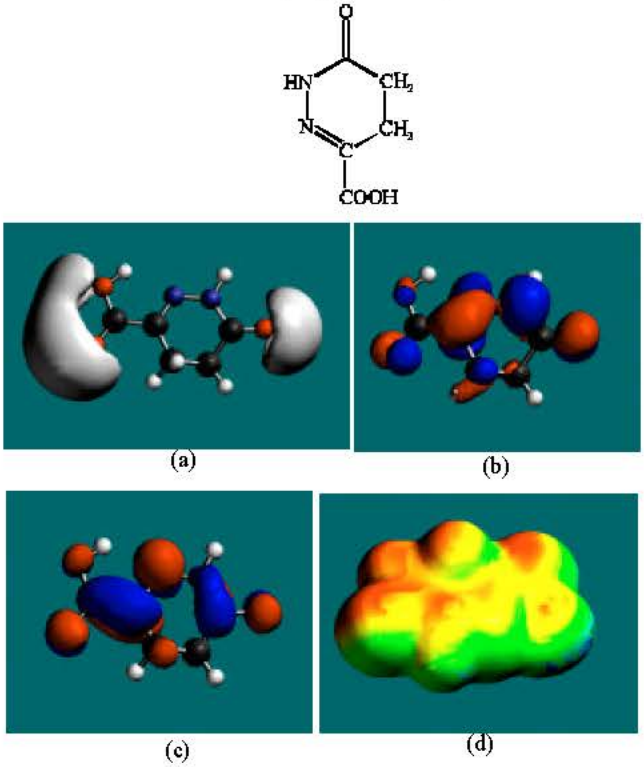

Fig. 8: Structure of THOPC giving the electrostatic potential in (a), HOMOs in (b), LUMOs in © and surface electric charges (where red indicates negative, blue indicates positive and green indicates neutral) in (d)

also, it is found to be more negative around the two carbonyl oxygen atoms and nitrogen atom of the pyridine ring, once again indicating that the positions may be subject to electrophilic attack. In the case of AcHD, the electrostatic potential is found to be more negative around the carbonyl oxygen atom and the primary amine nitrogen atom whereas in the case of HD the electrostatic potential is found to be more negative around both the amine nitrogen atoms, indicating that the positions may be subject to electrophilic attack. In the case of DAHD, the electrostatic potential is found to be more negative around both the amine nitrogen atoms.

In the case of INH, HOMOs with high electron density are found to be close to pyridine ring nitrogen atom, the two ring carbon atoms meta to the nitrogen atom, secondary amine nitrogen atom and the carbonyl oxygen atom whereas LUMOs are found close to all atoms except the primary amine nitrogen atom.

In the case of NAINH, HOMOs with high electron density and LUMOs are found to be close to all atoms of the pyridine ring, one amino nitrogen atom and carbonyl oxygen atoms whereas LUMOs are close all atoms of the pyridine ring. In the case of AcHD, HOMOs with high electron density and LUMOs are found close to amino nitrogen atoms, carbonyl oxygen atom and the methyl carbon atom. In the case of HD, HOMOs with high electron density and LUMOs are found close to two nitrogen atoms. In the case of DAHD, HOMOs with high electron density and LUMOs are found close to two amino nitrogen atoms and carbonyl oxygen atoms. In the case of PH, HOMOs with high electron density are found to be close to all non-hydrogen atoms except methyl carbon atom and LUMOs are found close to all non-hydrogen atoms.

Abundance of green, yellow and red regions with some blue patches on the surface of INH indicates the surface may have overall a small negative charge so that INH can undergo both dipole-

dipole and hydrophobic interaction with biomolecules. The surface of NAINH appears to predominate in yellow, red and green so that it will have an overall negative charge. The surface of AcHD predominates in red, yellow and green so that it will have an overall negative charge greater than that in the case of NANH. The surface of HD predominates in red, yellow and green so that it will have an overall negative charge greater than that in the case of AcHD. The surface of DAHD predominates in red, yellow and green so that it will have an overall negative charge greater than that in the case of NANH. The surface of PH predominates in red, yellow and green so that it will have an overall negative charge.

Conclusions

Molecular modelling analyses show that INH and its metabolites generally have large HOMO-LUMO energy differences and hence kinetically inert. PH and THOPC which have smaller LUMO-HOMO energy differences are expected to be more labile. Negatively charged nature of the surface of INH and a number of its metabolites indicates that the compounds may be subject to electrophilic attack. Large differences in heat of formation and entropy values suggest that AcHD, PH and THOPC may be spontaneously produced from HD.

Acknowledgments

Fazlul Huq is grateful to the School of Biomedical Sciences, The University of Sydney for the time release from teaching.

References

Arnadottir, T., 2001. Tuberculosis: Trends and twenty-first century. Scand. J. Infect. Dis., 33: 741-743.

Clark, D.W., 1985. Genetically determined variability in acetylation and oxidation. Therapeutic implications. Drugs, 29: 342-375.

Dye, C., S. Scheele, P. Dolin, V. Phathania and M.C. Raviglione, 1999. Consensus statement. Global burden of tuberculosis: Estimated incidence, prevalence and mortality by country, World Health Organization Global Surveillance and Monitoring Project. JAMA., 282: 677-686.

Eichelbaum, M., H.K. Kroemer and G. Mikus, 1992. Genetically determined differences in drug metabolism as a risk factor in drug toxicity. Toxicol. Lett. Spec., 64-65: 115-122.

Evans, D.A., K.A. Manley and V.A. McKusick, 1960. Genetic control of isoniazid metabolism in man. Br. Med. J., 2: 485-491.

Huq, F., 2006. Molecular modelling analysis of the metabolism of morphine. IJPAC, 2006, (accepted).

HyperCube HyperChem, 2002. Release 7 for Windows, 7.0 Ed.; HyperCube, Ed.

Kinzig-Schippers, M., D. Tomalik-Scharte, A. Jetter, B. Scheidel and V. Jakob, 2005. Should we use N-acetyltransferase type 2 genotyping to personalize isoniazid doses? Antimicrob. Agents Chemother., 49: 1733-1738.

Kochi, A., 1991. The global situation and the new control strategy of the World Health Organization. Tubercle, 72: 1-6.

Richards, V.E., B. Chau, M.R. White and C.A. McQueen, 2004. Hepatitic gene expression and lipid homeostasis in C57B1/6 mice exposed to hydrazine or acetylhydrazine. Toxicol. Sci., 82: 318-332.

Smith, C.M. and A.M. Reynard, 1992. Textbook of Pharmacology, W.B. Saunders, Philadelpia, USA., pp: 861-870.

Spartan '02, 2002. Wavefunction, Inc. Irvine, CA, USA.

WHO Report, 2002. Global Tuberculosis Control: Surveillance, Planning, Financing, World Health Organization, Geneva, WHO/CDS/TB/2002.295.